

## Lasers in Manufacturing Conference 2025

### Impact of polarization angle on ablation efficiency and structure formation in DLIP processing

Francisco Udo Marins Almeida<sup>a</sup>, Bogdan Voisiat<sup>a</sup>, Ignacio Tabares<sup>a</sup>, Fabian Ränke<sup>a</sup>, Andrés Fabian Lasagni<sup>a,b</sup>

*Technische Universität Dresden, George-Bähr Str. 3c, Dresden 01069, Germany*

*<sup>b</sup>Fraunhofer Institut for Material and Beam Technology, Winterbergstraße 28, Dresden 01277, Germany*

---

#### Abstract

Direct Laser Interference Pattering (DLIP) has evolved as an efficient method for surface functionalization by producing periodic structures. When using femtosecond or picosecond laser sources, the produced topographies are also covered by Laser Induced Periodic Surface Structures (LIPSS), being its orientation controlled by the polarization direction of the laser beam. On the other hand, their orientation has an effect not only on the geometry of the produced patterns, but also in the ablation efficiency during the structuring process. In this work, stainless steel 304 and aluminum 2024 plates are treated with 12 ps and 70 ps laser pulses (1064 nm) using DLIP, producing line-like structures with 6.0  $\mu$ m and 5.4  $\mu$ m periods. The polarization direction and thus the LIPSS orientation is controlled during the process. It was found that the ablation efficiency can be improved significantly when the LIPSS are perpendicular to the DLIP features, and that the line-like geometry of the DLIP features affects the expected orientation of the LIPSS.

**Keywords:** Direct Laser Interference Pattering; Laser Induced Periodic Surface Structures; Polarization control; Ablation efficiency.

---

#### 1. Introduction

Ultrashort pulsed lasers operating in the femtosecond and picosecond range have been reported to produce Laser Induced Periodic Surface Structures (LIPSS) in a large variety of materials, including metals, semiconductors and polymers. In addition, the orientation of the LIPSS is affected by the laser polarization, while their period is mostly affected by the used laser wavelength, as reported by Aguilar-Morales et al., 2019.

In the case of the Direct Laser Interference Pattering (DLIP) method, when ultra-short pulses are used, the produced features can also coexist with LIPSS. The principle of DLIP is based on the interference of two or more coherent laser beams, which generates a spatially periodic intensity pattern on the material surface. When two laser beams are used, line-like periodic structures are formed, and their spatial period can be controlled by adjusting the overlapping angle between the two beams. Furthermore, polarization of the laser beam has been found to influence the orientation of the LIPSS with respect to the DLIP features. For instance, Alamri et al. (2019) investigated the interplay between DLIP and LIPSS, demonstrating that the dominance of one structure over the other during formation depends on factors such as laser fluence and spatial period. Additionally, the polarization of the laser beam was found to influence whether the patterns form distinctly, overlap, or compete.

Although DLIP and LIPSS have been extensively studied as distinct surface structuring techniques, the effect of laser polarization direction on structure depth remains insufficiently explored. This study investigates the role of polarization in DLIP microstructuring by generating line-like patterns on stainless steel and aluminium using a two-beam DLIP setup with ultrashort laser pulses of 12 ps and 70 ps. The markedly different thermal properties of these materials enable a comparative analysis of heat conduction effects on polarization-driven structuring dynamics, as well as on the ablation efficiency of the process. Surface morphology and structure depth were characterized using White Light Interferometry (WLI) and Scanning Electron Microscopy (SEM).

## 2. Materials and Methods

Stainless steel 304 and aluminum 2024, with initial surface roughnesses of 8 nm and 196 nm, respectively, were cleaned with 99% ethanol and dried with compressed air. Two distinct DLIP systems were used, including (i) a 70 ps laser (neoMOS, neoLASE GmbH, Hannover, Germany) and (ii) a 12 ps laser (PX2003-GH, EdgeWave GmbH, Würselen, Germany), both operating at 1064 nm. An ELYPSIS optical head (SurFunction GmbH, Germany) splits the laser beam into two sub-beams, which are subsequently overlapped in a single elliptical spot. Interference periods of 5.4  $\mu$ m and 6.0  $\mu$ m were employed for the 70 ps and 12 ps pulses, respectively. The corresponding beam spot sizes were 61  $\mu$ m  $\times$  793  $\mu$ m and 136  $\mu$ m  $\times$  356  $\mu$ m. The beam polarization was controlled using a zero-order half-wave plate from 0° to 90° in 10° steps. A schematic representation of the used configurations was published by Marins Almeida et al., 2025.

Laser fluences of 1.1 and 1.7 J/cm<sup>2</sup> were used, and by adjusting the pulse-to-pulse overlap, accumulated fluences of 56.1 and 112 J/cm<sup>2</sup>, and 82.2 and 262 J/cm<sup>2</sup> were reached for the 12 ps and 70 ps pulses, respectively. The samples were irradiated in a single scan of 5 mm length, keeping all the other parameters constant.

The characterization of the laser-treated samples was done using a White Light Interferometer (Sensofar S Neox, Terrassa, Spain), performing three measurements for each combination of process parameters for statistical significance. Scanning Electron Microscopy (SEM) (Supra 40VP and Sigma 300 Gemini, Carl Zeiss, Germany) was performed at 3 to 5 kV. The SEM images were also analyzed in Fourier space to determine LIPSS spatial frequency and orientation.

## 3. Results

DLIP was used to produce line-like structures on both stainless steel 304 and aluminum 2024 alloys. The DLIP process permitted the creation of regular line-like surface patterns on both materials. On stainless steel (Figs. 1 a-d), also pronounced quasi-periodic LIPSS appeared alongside the laser-treated areas, including both Low and High Spatial Frequency LIPSS (LSFL, and HSFL, respectively). In case of aluminum, clear DLIP patterns were produced, but only LSFL features were visible with the 70 ps laser (Fig. 1 e, f) and absent with the 12 ps laser (Fig. 1 g, h). Rotation of the beam polarization (indicated as a double arrow in the figure) induced a change in the orientation of the LIPSS features. In general, this type of LIPSS are perpendicular to the polarization direction. The FFT analysis in the orange insets of Fig. 1 shows that LIPSS orientation angles deviate in some cases from the expected orientation (perpendicular to the polarization direction). These deviations reach up to 12° in Fig. 1 a-c, and 32° in Fig. 1d.

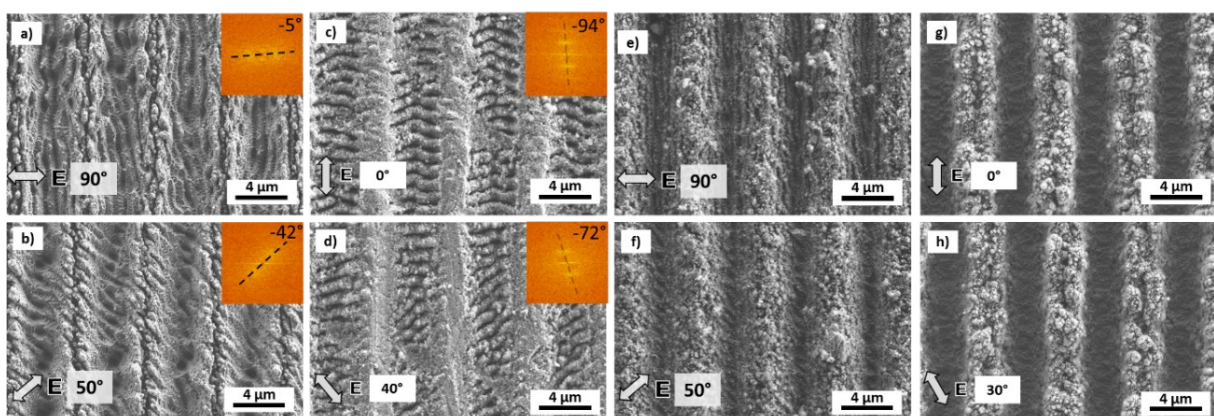


Figure 1. SEM images of DLIP structured surface on steel 304 at 70 ps (a, b) and 12 ps (c, d), as well as on aluminum 2024, irradiated at 70 ps (e, f) and 12 ps (g, h). Fourier transforms of the SEM images are included as inset. The polarization direction is indicated by the double arrow. Modified from Marins Almeida, F.U., Voisiat, B., Tabares, I., Ränke, F., Lasagni, A.F. Influence of polarization angle on LIPSS formation and ablation efficiency in direct laser interference patterning of metals, Sci. Rep. 15, 20285 (2025), under Creative Commons Attribution 4.0 International License (<https://doi.org/10.1038/s41598-025-07657-4>).

This high discrepancy led to further investigation by plotting the LIPSS angle as a function of the polarization, as shown in Figure 2. The black dashed line indicates ideal perpendicularity between laser beam polarization and the LIPSS orientation. However, significant differences are observed. In the case of steel (Fig. 1a), between 0° and 40° polarization, the LIPSS rotate only 22°, resulting in a 18° difference from the expected alignment. This suggests that the DLIP lines influence the LIPSS orientation, reducing their rotation relative to the polarization direction. At larger polarization angles, the trend reverses. For example, at a 70° polarization angle, the LIPSS are oriented at ~0° (20° difference compared to the expected orientation).

This behavior was observed for both pulse durations (Fig. 1a), further confirming the influence of DLIP structures on LIPSS alignment.

In the case of aluminum 2024, the observed behavior of the LIPSS was slightly different (Fig. 1b). Firstly, the samples irradiated with 12 ps did not present LIPSS. In case of the 70 ps pulses, the LSFL remained nearly perpendicular to DLIP between 0° and 40° polarization angles. Beyond 40°, LIPSS shifted, aligning mostly orthogonally with the polarization angle. This behavior is likely due to aluminum's high thermal conductivity and weaker electron-phonon coupling, which disrupts pattern formation. LSFL orientation arises from light-matter interaction, where laser-induced surface plasmon polaritons (SPPs) propagate along the polarization direction. As the polarization angle changes, so does the SPP propagation relative to the DLIP. Surface features affect LSFL formation by introducing directional scattering and altering local field enhancement (Gallego et al., 2025; Preusch et al., 2016). Around 50°, an equilibrium between polarization-driven plasmonic effects and surface-guided scattering may align LIPSS closer to perpendicularity. Rougher surfaces ( $SA > 200$  nm) have been shown to dominate over laser polarization, exerting greater influence on LIPSS orientation (Sotelo et al., 2023).

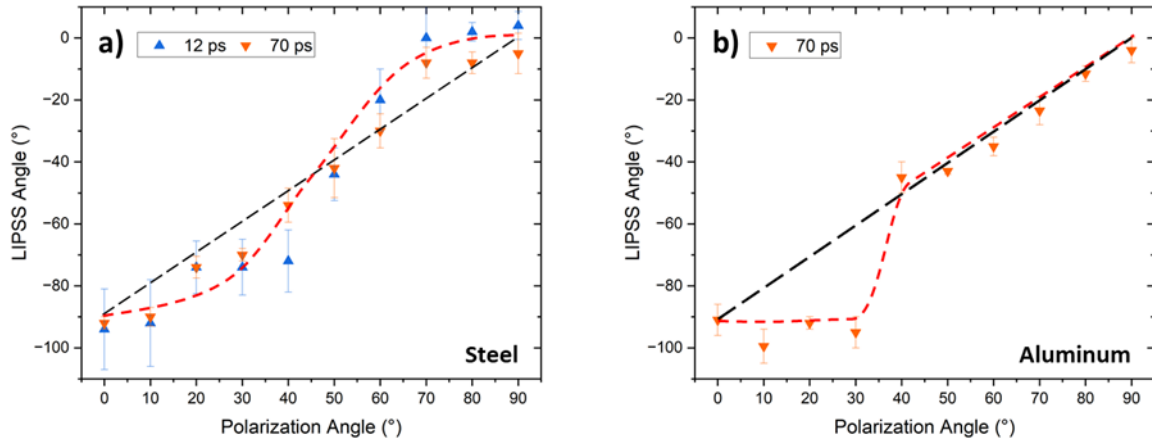


Figure 2. LIPSS orientation angle as a function of the polarization angle for 12 ps and 70 ps pulses in (a) stainless steel 304 and (b) aluminum 2024. The black dashed line indicates ideal perpendicularity. Modified from Marins Almeida, F.U., Voisiat, B., Tabares, I., Ränke, F., Lasagni, A.F. Influence of polarization angle on LIPSS formation and ablation efficiency in direct laser interference patterning of metals, *Sci. Rep.* 15, 20285 (2025), under Creative Commons Attribution 4.0 International License (<https://doi.org/10.1038/s41598-025-07657-4>).

Subsequent to the previous analysis, the effect of polarization on DLIP structure depth was also investigated by means of White Light Interferometry (WLI). The obtained topographical images show that the depth of the DLIP line-like patterns varies with LIPSS orientation, and thus impacts process efficiency (see Figs. 3b and 3d). Exemplary images for both materials are shown in Figs. 3a and 3b.

For example, in stainless steel 304 (Fig. 3b), irradiated at  $56.1 \text{ J/cm}^2$  with 12 ps pulses, the structure depth ranged from  $2.4 \mu\text{m}$  to  $3.7 \mu\text{m}$ , which means that ablation is 54% more efficient when the LIPSS are perpendicular to DLIP lines. For aluminum (also irradiated under the same conditions), the depth varied from  $10.6 \mu\text{m}$  to  $7.7 \mu\text{m}$ , meaning a 27% difference. Also in this case, the ablation efficiency was higher with the LSFL were aligned perpendicularly to the DLIP lines.

Compared to the 12 ps treatment, the obtained structure depth at 70 ps was significantly lower (even when applying high cumulated fluences). In addition, at low fluences, the measured depths remain nearly constant. For example, in the case of aluminum 2024 irradiated at  $82.2 \text{ J/cm}^2$ , the structure depth was  $\sim 0.75 \mu\text{m}$ . For steel, it was  $\sim 0.80 \mu\text{m}$ . For the last material, a slight improvement in the ablation efficiency was observed when irradiating at  $262.0 \text{ J/cm}^2$ . In this case, the structure depth was  $\sim 2 \mu\text{m}$  for the condition in which the LSFL were perpendicular to the DLIP lines, while  $\sim 1.5 \mu\text{m}$  for the parallel condition.

In case of the aluminum surface treated with 12 ps pulses at  $112.0 \text{ J/cm}^2$ , a different behavior was observed. In this case, the line-like structures were deeper ( $\sim 10.5 \mu\text{m}$ ) when the LSFL were parallel to the DLIP lines (e.g., the structure depth was  $\sim 5.9 \mu\text{m}$  for a polarization angle of  $0^\circ$ ). However, excessive ablation was observed for this condition, which led to significant re-deposition of material and thus decreased the apparent structure depth. This effect has been confirmed recently by Ränke et al., 2025, employing Focus Ion Beam cross-sectional analysis. Further information can be found in Marins Almeida et al., 2025.

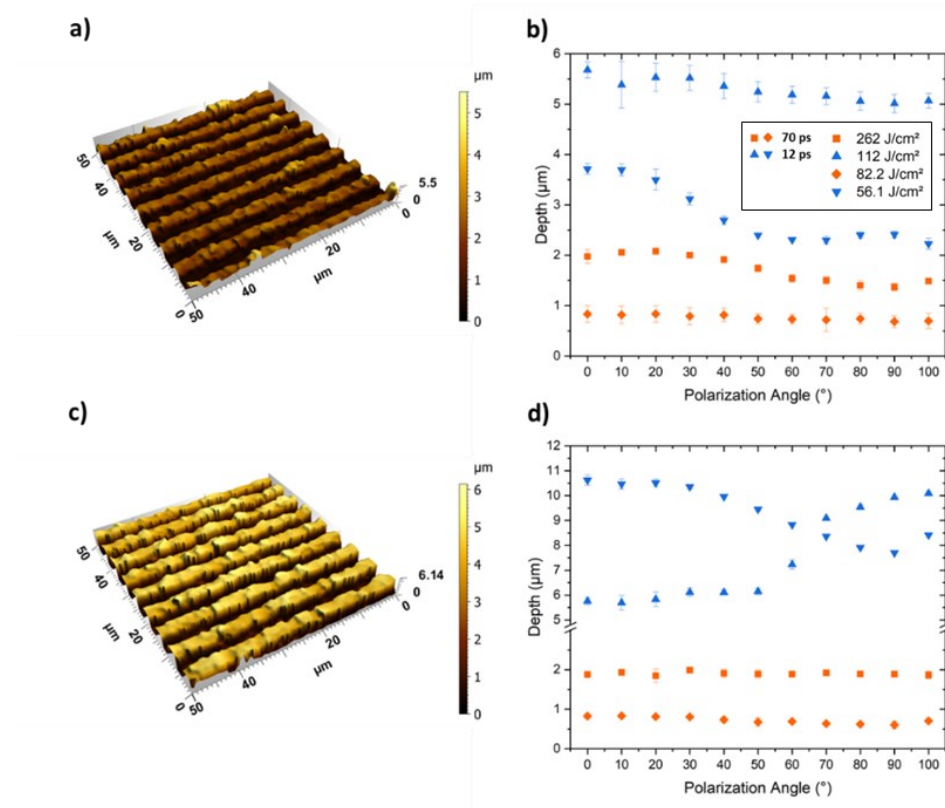


Figure 3. WLI surface profiles and structure depth evolution as function of beam polarization angle for (a, b) steel and (c, d) aluminum. Modified from Marins Almeida, F.U., Voisiat, B., Tabares, I., Ränke, F., Lasagni, A.F. Influence of polarization angle on LIPSS formation and ablation efficiency in direct laser interference patterning of metals, Sci. Rep. 15, 20285 (2025), under Creative Commons Attribution 4.0 International License (<https://doi.org/10.1038/s41598-025-07657-4>).

#### 4. Conclusions

DLIP structuring of aluminum 2024 and stainless steel 304 was studied using 12 ps and 70 ps pulses at 1064 nm under varying polarization angles. The main conclusions of this study include:

- i- Stainless steel exhibited both LSFL and HSFL on DLIP-patterned surfaces, while in Al 2024 only LSFL were observed for the 70 ps pulses.
- ii- Polarization direction influenced LSFL orientation, with a sharp reorientation up to 40-50°, indicating competition between DLIP and LIPSS formation mechanisms, especially for stainless steel 304.
- iii- Structure depth varied with polarization, with deeper features when LIPSS were perpendicular to DLIP lines, especially in stainless steel.
- iv- Excessive ablation led to material redeposition, which reduced the effective structure depth by partially masking the DLIP-patterned lines.

These findings underline the importance of polarization and material properties in controlling DLIP-induced surface morphology.

#### Acknowledgements

This project was funded by the Federal Ministry for Economic Affairs and Climate Action (BMWK) of Germany, project number KK5058306SY3 within the framework of the Central Innovation Programme for small and medium-sized enterprises (ZIM). The authors acknowledge the fruitful discussion with Prof. Antonio Ancona (University of Bari, Italy) and Prof. Gert-Willem Romer (Twente University, The Netherlands).

## References

Alamri, S., Fraggelakis, F., Kunze, T., Krupop, B., Mincuzzi, G., Kling, R., Lasagni, A.F., 2019. "On the interplay of DLIP and LIPSS upon ultra-short laser pulse irradiation". *Materials* 12, p. 1018. <https://doi.org/10.3390/ma12071018>

Aguilar-Morales, A.I., Alamri, S., Voisiat, B., Kunze, T., Lasagni, A.F., 2019. "The role of the surface nano-roughness on the wettability performance of microstructured metallic surface using direct laser interference patterning". *Materials* 12, p. 2737. <https://doi.org/10.3390/ma12172737>.

Gallego, D., Ayerdi, I., Pan, A., Olaizola, S.M., Rodriguez, A., 2025. "The role of unidirectional surface roughness on the regularity of LIPSS generated on stainless steel using femtosecond lasers". *Scientific Reports* 15, p. 15483. <https://doi.org/10.1038/s41598-025-00185-1>

Marins Almeida, F.U., Voisiat, B., Tabares, I., Ränke, F., Lasagni, A.F., 2025. "Influence of polarization angle on LIPSS formation and ablation efficiency in direct laser interference patterning of metals". *Scientific Reports* 15, p. 20285. <https://doi.org/10.1038/s41598-025-07657-4>

Preusch, F., Rung, S., Ralf, H., 2016. "Influence of polishing orientation on the generation of LIPSS on stainless steel". *Journal of Laser Micro/Nanoengineering* 11, pp. 137–142. <https://doi.org/10.2961/jlmn.2016.01.0025>

Ränke, F., Salles, M., Soldera, M., Tabares, I., Soldera, F., Lasagni, A.F., 2025. "Optimized strategy for fabricating high-aspect-ratio periodic structures over large areas using ps-direct laser interference patterning". *Advanced Engineering Materials*, n/a, p. 2500570. <https://doi.org/10.1002/adem.202500570>

Sotelo, L., Fontanot, T., Vig, S., Fernandes, M.H., Sarau, G., Leuchs, G., Christiansen, S., 2023. "Initial surface roughness influence on the generation of LIPSS on titanium and stainless steel and their effect on cell/bacteria viability", in: *Laser-Based Micro- and Nanoprocessing XVII*. Presented at the *Laser-Based Micro- and Nanoprocessing XVII*, SPIE, pp. 137–154. <https://doi.org/10.1117/12.2648921>